ARTICLE
Journal of Cellular Biochemistry 113:1022–1033 (2012)

Journal of Cellular Biochemistry

Triptolide Attenuate the Oxidative Stress Induced by LPS/D-GalN in Mice

Yan Lu, Xiaofeng Bao, Tingzhe Sun, Jiafa Xu, Wei Zheng, and Pingping Shen*

State Key Laboratory of Pharmaceutical Biotechnology, and Model Animal Research Center (MARC) of Nanjing University, Nanjing University, Nanjing 210093, China

ABSTRACT

Triptolide, a diterpene triepoxide, is one of the major components of most functional extracts of *Tripterygium wilfordii Hook f*, which is known to have various biological effects, including immunosuppressive, anti-inflammatory and anti-tumor functions. We studied the inhibitory effect of triptolide on endotoxemia (ETM)-induced oxidative stress, which was induced in C57BL/6 mice by lipopolysaccharide (LPS) and D-galactosamine (D-GalN). Pretreatment with triptolide decreased the reactive oxygen species (ROS) levels, mortality rate and liver injury after LPS/D-GalN injection. We utilized comprehensive proteomics to identify alterations in liver protein expression during pretreatment with triptolide or *N*-acetylcysteine (NAC) after LPS/D-GalN injection, 44 proteins were found to be related to oxidative stress, mitochondria, metabolism and signal transduction, and 23 proteins of them seemed to be significantly up- or down-regulated. Furthermore, both triptolide and NAC inhibited activation of c-jun NH2-terminal kinases (JNK) and mitogen-activated protein kinase p38 (p38), phosphorylation of inhibitor of nuclear factor-kappa B (IκB) and activation of nuclear factor-κB (NF-κB). These results demonstrated that triptolide inhibited the activation of JNK and p38 by decreasing ROS levels, which in turn inhibited the hepatic injury. In addition, we set and validated the phosphorylation model of extracellular signal-regulated kinase (ERK) and proposed that triptolide probably induced ERK phosphorylation through inhibiting its dephosphorylation rates. These results showed that triptolide can effectively reduce the oxidative stress and partially rescue the damage in the liver induced by LPS/D-GalN. J. Cell. Biochem. 113: 1022–1033, 2012.

KEY WORDS: TRIPTOLIDE; OXIDATIVE STRESS; LIVER INJURY; PROTEOMICS

Extracts of the root of Tripterygium wilfordii Hook f (TWHf) have been used in traditional Chinese medicine for the treatment of a variety of autoimmune diseases such as rheumatoid arthritis, nephritis, systemic lupus erythematosus, psoriasis, and dermatomyositis for centuries [Brinker et al., 2007]. Triptolide, a diterpene triepoxide, is one of the major components of most functional extracts of TWHf and is known to have immunosuppressive and anti-inflammatory properties [Ma et al., 2007], including prolonging allograft survival [Ji et al., 2006], therapy for rheumatoid arthritis and nephritis [Qiu and Kao, 2003], and anti-fertility and anti-tumor effects [Wang et al., 2007].

Recently, several studies revealed that the effects of triptolide were correlated with its activity in the regulation of oxidative stress imbalance [Zheng et al., 2008]. Xue et al. [2006] demonstrated that triptolide protected PC-12 cell from hydrogen peroxide-induced cell death, and that the underlying mechanism might be related to its inhibitory effect on the transcription activity of nuclear factor-κB (NF-κB). In our previous report, we revealed that triptolide exhibited a suppressive effect on macrophages and suppressed the generation of reactive oxygen species (ROS) and NO, which in turn suppressed NF-κB activation and multiple proinflammatory cytokines gene expressions, suggesting that triptolide had anti-inflammatory and immunosuppressive effects [Wu et al., 2006].

Abbreviations used: D-GalN, D-galactosamine; DHR, dihydrorhodamine 123; ERK, extracellular signal-regulated kinase; ETM, endotoxemia; GSH, reduced glutathione; IHC, immunohistochemiscal assay; IκB, inhibitor of nuclear factor-kappa B; JNK, c-jun NH2-terminal kinase; LPS, lipopolysaccharide; MAPK, mitogen-activated protein kinase; MKK, MAPK kinase; MKKK, MKK kinase; MKKKK, MKKK kinase; NAC, *N*-acetylcysteine; NF-κB, nuclear factor-κB; ROS, reactive oxygen species; p38, mitogen-activated protein kinase p38; TWHf, Tripterygium wilfordii Hook f.

The authors declare that there are no conflicts of interest.

Yan Lu and Xiaofeng Bao contributed equally to this work.

Grant sponsor: National Natural Science Foundation of China; Grant numbers: 81001665, 91013015, 30821006, 30870588; Grant sponsor: National Key Basic Research Program of China; Grant number: 2010CB912203.

*Correspondence to: Pingping Shen, State Key Laboratory of Pharmaceutical Biotechnology, and Model Animal Research Center (MARC) of Nanjing University, Nanjing University, Nanjing 210093, China.
E-mail: ppshen@nju.edu.cn

Received 19 August 2011; Accepted 25 October 2011 • DOI 10.1002/jcb.23434 • © 2011 Wiley Periodicals, Inc.
Published online 7 November 2011 in Wiley Online Library (wileyonlinelibrary.com).

The severe liver injury induced by lipopolysaccharide (LPS) and D-galactosamine (D-GalN) is a well-established model of oxidative stress-mediated liver injury [Morikawa et al., 2004; Nogueira et al., 2009; Savegnago et al., 2009]. The production of ROS, detected by immunohistochemical and biochemical methods in the severe liver injury, can initiate a wide range of toxic oxidative reactions [Han et al., 2006]. Overall, oxidative stress and subsequent free radical formation appear to play a crucial part in severe liver injury [Schwabe and Brenner, 2006].

In this study, we found that triptolide pretreatment attenuates oxidative stress in LPS/D-GalN challenged severe liver injury mouse model. Proteomic analysis showed that triptolide pretreatment recovered the destroyed anti-oxidant defense system in this model. Our data indicated that triptolide evidently enhances anti-oxidant system and reduces the ROS lever in liver. Furthermore, we examined a sequence of molecular events that mediates the induction of liver injury through ROS. In brief, triptolide inhibited activation of c-jun NH2-terminal kinase (JNK) and mitogen-activated protein kinase p38 (p38), phosphorylation of inhibitor of nuclear factor-kappa B (IκB) and activation of NF-κB through attenuating the increased ROS generation in livers and other place. In addition, combining mathematical model and conventional experiments, we validated the phosphorylation model of extracellular signal-regulated kinase (ERK). We proposed that triptolide probably induces ERK phosphorylation through inhibiting its dephosphorylation rates. Collectively, these results demonstrate that triptolide is able to rescue severe liver injury by reducing oxidative stress in livers.

MATERIALS AND METHODS

ANIMAL MODEL

Male C57BL/6 mice (6–8 weeks old, weighing 22–25 g) were obtained from the Model Animal Research Center of Nanjing University, Nanjing. On arrival, mice were randomized and transferred to plastic cages containing saw dust bedding (five mice per cage), given food and water ad libitum, and maintained under pathogen-free conditions. Animal welfare and experimental procedures were carried out in strict accordance with the Guide for the Care and Use of Laboratory Animals (The Ministry of Science and Technology of China, [2006]-398) and the related ethical regulations of our university. The protocol was approved by the State Key Laboratory of Pharmaceutical Biotechnology in Nanjing University (Number of Permit Date: 20070521), and all efforts were made to minimize suffering.

Severe liver injury was induced in mice by an intravenous injection (i.p.) coinjection of LPS (5 μg/kg of body weight) and D-GalN (400 mg/kg of body weight) [Galanos et al., 1979]. Triptolide was administered intragastrically (i.g.) in a single dose (5 μg/kg of body weight) at 12 h before subsequent coinjection with LPS and D-GalN. *N*-acetylcysteine (NAC) was dissolved in normal saline (NS) and administered in a single i.p. dose (150 mg/kg of body weight) at 1 h before injection with LPS and D-GalN [Wiesel et al., 2000]. The mice of vehicle-pretreated group (n = 6) were administered intragastrically (i.g.) with 2.5 μl/kg DMSO, 0.1% in normal saline at 12 h before subsequent coinjection with LPS and D-GalN.

REAGENTS

Crystalline triptolide (PG490, molecular weight 360) was obtained from Alexis (Carlsbad, CA). Triptolide was dissolved in dimethyl sulphoxide (DMSO) and stored at 2 mg/ml at −20°C. Triptolide was freshly diluted with normal saline (NS) to the indicated concentrations before use (the final concentration of DMSO did not exceed 0.1% (v/v)). Antibodies against inhibitor IκB, JNK, ERK, and p38 were purchased from Cell Signaling Technology (Beverly, MA). All other chemicals were purchased from Sigma Chemicals, Inc., unless otherwise stated.

HISTOLOGY AND IMMUNOHISTOCHEMISTRY

Liver tissue was fixed in 4% formalin solution and embedded in paraffin. Paraffin sections were cut at 5 μm thickness, dewaxed, and stained with hematoxylin and eosin for histological analysis, which was evaluated for morphologic changes by light microscopy.

For p-IκB and p-JNK immunohistochemistry, dewaxed sections were boiled for 10 min in 10 mM citrate, pH6.0, in a pressure cooker to retrieve antigen. After cooling, sections were rinsed in Tris-buffered saline containing 0.1% Tween 20 (TBST) and incubated in 3% H_2O_2 for 5 min. Then the liver sections were incubated with goat serum to prevent non-specific binding, and stained with antibody for mouse p-IκB or p-JNK for 1 h at room temperature. After rinsing with TBST, the sections were then incubated with horseradish peroxidase (HRP)-conjugated goat anti-rabbit IgG (Zymed Laboratories, Inc.) for 15 min at room temperature. Finally, the sections were developed by DAB, and counterstained with hematoxylin, and mounted.

SERUM ALANINE AMINOTRANSFERASE (ALT) AND ASPARTATE AMINOTRANSFERASE (AST) ASSAY

Serum was collected at 2, 4, and 5 h after coinjection with LPS and D-GalN. Serum ALT and AST activities were determined by ALT and AST kit according to the manufacturer's instruction (Shanghai Rongsheng, Shanghai, China).

PROTEOMICS

Proteomics analysis of liver protein sample was conducted according to the established procedure described previously [Chen et al., 2005]. In brief, Proteins of whole livers from four groups (three mice in each group) including negative control (replace LPS/D-GalN administration by NS), positive control (with LPS/D-GalN), triptolide pretreatment and NAC pretreatment were rinsed twice with ice-cold PBS, homogenized, and then suspended in at least 3 volumes of ice-cold ethanol. The protein in each sample was then precipitated at −30°C for 2 h and pelleted at 15,000*g* at 4°C for 30 min. The protein pellet was rinsed twice with ice-cold ethanol and then dissolved in rehydration buffer containing 7 M urea, 2 M thiourea, 2% (w/v) CHAPS, 65 mM DTT, and 0.5% IPG buffer (Amersham Biosciences). The protein concentration was determined by the Bradford method.

2-DE. Three gels per sample were processed and analyzed simultaneously. The first dimension was carried out on an Ettan IPGphor II isoelectric focusing unit (Amersham Biosciences) using 24-cm pH 3–10 IPG gel strips and 450 μl of sample solution. IEF was performed at 20°C under the following conditions: 12 h at 30 V, 30 min at 300 V, 1 h at 500 V, 1 h at 1,000 V, 2 h at 5,000 V, and 8 h at 8,000 V. After IEF, the IPG strips were immediately equilibrated two successive times for 15 min each in SDS equilibration buffer containing 50 mM Tris–HCl, pH 6.8, 30% glycerol (Amresco), 1% SDS (Amresco), and traces of bromophenol blue. The first equilibration was performed in the above mentioned equilibration buffer with 1% (w/v) DTT followed by a second equilibration with 2.5% (w/v) iodoacetamide. The gels were subsequently subjected to a second dimensional electrophoresis on 12.5% polyacrylamide gels using an Ettan Daltsix electrophoresis system (Amersham Biosciences). SDS–PAGE was performed at 2 W/gel for 45 min and 15 W/gel for about 5 h until the dye front reached the bottom of the gels. Finally proteins on the 2-DE gels were visualized with Coomassie Brilliant Blue R-250.

Gel image and data analysis. The Coomassie Blue-stained gels were scanned on a Sharp JX-330 color image scanner. Spot detection, quantification, and matching were performed with PDQuest software (Bio-Rad). Proteins separated by 2-DE gels were quantitated in terms of their relative volume (percent volume). This relative volume was calculated by dividing the individual spot volume by the sum of total spot volumes and then multiplying by 100. The expression levels of proteins with 1.5 times increase or 50% decrease as compared with the control were considered significantly changed.

In-gel tryptic digestion of proteins. Spots were cut out of 2-D gels, sliced into small pieces, and washed twice with 50% acetonitrile (Fisher) in 25 mM ammonium bicarbonate. The gel pieces were dried in a vacuum centrifuge. The proteins were digested overnight with 10 ng/μl trypsin (sequencing grade, Promega Benelux, Leiden, The Netherlands) at 37°C. The peptide fragments were extracted twice with 5 μl of water/acetonitrile/formic acid (5:14:1). After drying in a vacuum centrifuge, the lyophilized digest was dissolved in 0.1% (v/v) TFA.

MALDI-TOF mass spectrometry and protein identification. The trypsin-digested sample was mixed with the matrix (((α)-cyano-4-hydroxycinnamic acid) dissolved in 0.1% TFA of 50% acetonitrile aqueous solution) and then analyzed using the Ultraflex TOF/TOF mass spectrometer system (Bruker). Mass spectra were recorded in the positive ion mode with delayed extraction. Monoisotopic masses of peptides were analyzed using the Mascot search engine. Mass spectra data were searched in SWISS-PROT (database).

LIVER ROS DETERMINATION

The levels of ROS in liver were detected by using the fluorescence probe dihydrorhodamine 123 (DHR). Liver tissue (50 mg) was homogenized in 1 ml well-oxygenated buffer (150 mM KCl, 20 mM Tris, 0.5 mM EDTA, 1 mM $MgCl_2$, 5 mM glucose, 0.5 mM octanoic acid, pH 7.4) with a glass homogenizer in an ice bath. DHR (0.5 μl of 10 mM) was added to the homogenate and incubated at 37°C for 30 min. After centrifuging at 6,000*g* at 4°C for 5 min, the fluorescence intensity of supernatant was measured at an excitation wavelength of 500 nm and an emission of 536 nm by using a fluorescent Mutilabel Counter (Safire, TECAN, Austria). The relative amount of ROS level was expressed as the fluorescence ratio of the treatment to control.

WESTERN BLOTTING

Liver tissue (50 mg) was homogenized in 1 ml lysis buffer (50 mM Tris, 150 mM NaCl, 5 mM EDTA, 0.1% SDS, 1 mM DTT, 1 mM PMSF, PH 7.4) with a glass homogenizer in an ice bath. The proteins (30 μg per sample) were electrophoresed on 12% sodium dodecyl sulfate polyacrylamide gels (SDS–PAGE), and then electrotransferred onto a polyvinylidene fluoride (PVDF) membrane (Amersham, UK). The detection step was performed with HRP-conjugated antibody. The target proteins were visualized with an Enhanced Chemiluminescent Method kit (SABC, PRC).

ELECTROPHORETIC MOBILITY SHIFT ASSAY (EMSA)

Nuclear protein from liver tissue (50 mg) was extracted as previously described [Tsai et al., 2000], and was stored at −70°C before use. Two double stranded oligonucleotide probes containing a consensus binding sequence for NF-κB (5′-AGT TGA GGG GAC TTT CCC AGG C-3′) were 3′ end-labeled with DIG. EMSA experiments were performed as described previously [KretzRemy et al., 1996].

HOECHST STAINING

Paraffin sections prepared above was deparaffinized in three changes of xylene followed by rehydration in a graded alcohol series. Slides were then rinsed and immersed in 0.2 μg/ml Hoechst 33345 (Sigma Chemicals, Inc.) in the dark for 10 min. After thorough washing in PBS, nuclear Hoechst-stained DNA was then observed and evaluated for morphologic changes by fluorescence microscopy. Imaging was performed using a Nikon E80i microscope (Nikon, Tokyo, Japan).

STATISTICAL ANALYSIS

Data were expressed as the mean ± standard error (SE). Statistical analysis was performed by the Student's *t*-test when only two value sets were compared, and one-way ANOVA followed by Dunnett's test when the data involved three or more groups. The log-rank test was performed for survival curve. $P < 0.05$, $P < 0.01$, or $P < 0.001$ was considered statistically significant and indicated by *, **, or ***, respectively.

MATHEMATICAL MODELING

We adopted a simplified model developed by Kholodenko [2000]. The temporal dynamics was represented by a set of ordinary differential equations which were described in detail with moiety conservation laws in Tables I and II. Parameter values were modestly adjusted to qualitatively describe our experimental data. Deterministic equations were numerically integrated with MATLAB (The MathWorks, Natick, MA, Version 7, Release 14) built-in solver ode23s [Kholodenko, 2000].

TABLE I. The Biological Meanings of the Abbreviations Found in the Equations

Abbreviations	Biological interpretation
MAPK	Mitogen-activated protein kinase
MAPK-P	Monophosphorylated MAPK
MAPK-PP	Biphosphorylated MAPK
MKK	MAPK kinase
MKK-P	Monophosphorylated MKK
MKK-PP	Biphosphorylated MKK
MKKK	MKK kinase
MKKK-P	Monophosphorylated MKKK

RESULTS

TRIPTOLIDE ATTENUATED SEVERE LIVER INJURY INDUCED BY LPS/D-GaLN

In previous studies, Mignon et al. [1999] found that challenge with 5 μg/kg LPS and 400 mg/kg D-GalN in mice resulted in severe liver injury and a high mortality in a short time. So we established this disease model to examine the anti-oxidant effects of triptolide on severe liver injury: a single i.g. dose of triptolide (5 μg/kg of body weight) was administered at 12 h before subsequent coinjection with LPS and D-GalN. Safe and effective dose of triptolide was determined according to the Bureau of Chinese Medicine Administration [Li et al., 2004]. As shown in Figure 1A, triptolide pretreatment attenuated LPS/D-GalN induced mortality. Three mice (33.3%) survived for more than 6 h after LPS/D-GalN treatment as compared to the untreated control. The protective effect of triptolide was also confirmed as the elevation of serum ALT and AST levels in triptolide-pretreated mice which was significantly lower than the untreated mice following intoxication (Fig. 1B,C). Furthermore, histological analysis showed that liver cell necrosis and local infiltration of inflammatory cells declined significantly and that hepatic congestion was relieved by triptolide, indicating that triptolide pretreatment reduced hepatocyte destruction induced by LPS/D-GalN intoxication (Fig. 2). Moreover, the result from vehicle pretreated group indicated that the i.g. treatment with vehicle cannot protect liver cell from oxidative stress.

TABLE II. Ordinary Differential Equations and Parameters

$J_1 = k_1\ [MKKK]/((1 + ([MAPK - PP]/K_I)^n)\ (K_1 + [MKKK]))$[a]
$J_2 = k_2\ [MKKK - P]/(K_2[MKKK - P])$
$J_3 = k_3\ [MKKK - P]\ [MKK]/(K_3[MKK])$
$J_4 = k_4\ [MKKK - P]\ [MKK - P]/(K_4 + [MKK - P])$
$J_5 = k_5\ [MKK - PP]/(K_5 + [MKK - PP])$
$J_6 = k_6\ [MKK - PP]/(K_6 + [MKK - PP])$
$J_7 = k_7\ [MKK - PP]\ [MAPK]/(K_7 + [MAPK])$
$J_8 = k_8\ [MKK - PP]\ [MAPK - P]/(K_8 + [MAPK - P])$
$J_9 = k_9\ [MAPK - PP]/(K_9 + [MAPK - PP])$
$J_{10} = k_{10}\ [MAPK - P]/(K_{10} + [MAPK - P])$
With parameters:
$k_1 = 15$, $n = 2$, $K_I = 18$, $K_1 = 50$, $k_2 = 2$, $K_2 = 40$, $k_3 = 0.2$,
$k_7 = 0.2$, $K_7 = 100$, $k_8 = 0.2$, $K_8 = 100$, $k_9 = 8$, $K_9 = 100$, $k_{10} = 8$, $K_9 = 100$
In TP treated simulation, k_9 and k_{10} are both set 2

[a]In our model, MAPK-PP donates the level of P-Erk (see corresponding figures). Species concentrations are expressed in nM. Catalytic rate constants and maximal rate constants are represented in min^{-1} and $nM\,min^{-1}$, respectively.

ROS IS INVOLVED IN LPS\D-GALN INDUCED LIVER INJURY

Next, we verified whether oxidative stress was involved in LPS/D-GalN induced severe liver injury. In order to test this hypothesis, we used fluorescence probe DHR to measure the changes of ROS in mice's livers after LPS/D-GalN intoxication. Relative levels of ROS were expressed as the fluorescence intensity ratio of the treated groups to the control (the untreated group). As shown in Figure 3, the ROS levels in treated livers were increased by 170% as compared to livers from control mice at 5 h, and this increment was up to 240% at 6 h, demonstrating that severe liver injury was accompanied by increase in ROS level in these livers.

To further confirm the involvement of ROS in severe liver injury, anti-oxidant NAC was used to perturb the generation of ROS in mice's livers. As seen in Figure 3, the enhanced ROS levels in damaged livers were suppressed by the pretreatment with a single i.p. of 150 mg/kg NAC 1 h before LPS/D-GalN intoxication. At 5 h, the ROS level in liver was decreased by 49.8% relative to positive control (LPS/D-GalN intoxication group), and at 6 h the ROS level was decreased by 34.9%. After NAC pretreatment, the survival rate rose from 0% to 33.0% after 6 h of intoxication (Fig. 1A). The protective effect of NAC was also confirmed by the results that NAC pretreatment decreased elevation of serum ALT and AST levels in intoxicated mice (Fig. 1B,C). Furthermore, histological analysis showed that intrahepatic hemorrhage and destruction of liver structure induced by LPS/D-GalN intoxication was significantly attenuated by NAC pretreatment (Fig. 2A,B). Conclusively, these data revealed that ROS was involved in severe liver injury induced by LPS/D-GalN. Moreover, the results shown in Figure 3 indicated that the i.g. with vehicle cannot change ROS lever in severe liver injury.

TRIPTOLIDE ATTENUATED SEVERE LIVER INJURY BY SUPPRESSING ROS PRODUCTION IN LIVER

Since triptolide effectively mitigate severe liver injury, and ROS played a role in these injuries (Fig. 3), it is possible that reduction in liver injury by triptolide was associated with its effect on suppressing the production of ROS in livers. To investigate this possibility, we measured the ROS levels in triptolide-pretreated mice's livers after LPS/D-GalN intoxication. As shown in Figure 3, the ROS levels in mice's liver were clearly reduced after triptolide pretreatment. At 5 h, the ROS level in liver was decreased by 42.7% contrast to positive control, and at 6 h the ROS level was decreased by 35.2%. These results indicated that salvage effect of triptolide on severe liver injury was associated with its effect on suppressing ROS production in liver.

LIVER PROTEIN VARIATION PROFILES WERE OBTAINED USING PROTEOMICS

In order to identify the molecular evidence for the protective effect of triptolide on oxidative stress injury, we utilized proteomics analysis to detect alterations of liver protein expressions, especially the proteins involved in anti-oxidant system. The proteomes of the four groups, including negative control (three mice), LPS plus D-GalN treated group (three mice), triptolide pretreated (three mice), and NAC pretreated group (three mice), were compared using 2-DE. Figure 4A showed four representative 2-D gel images of the protein

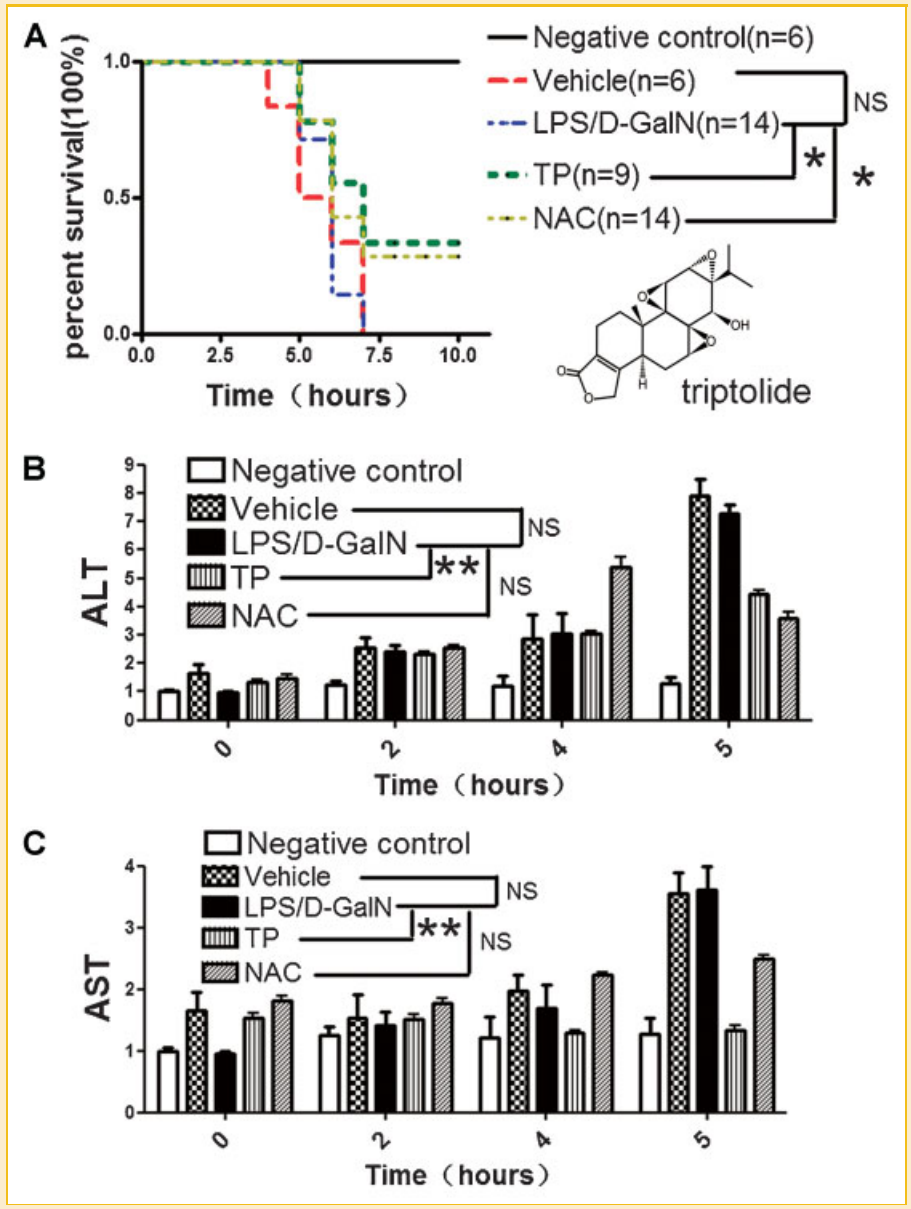

Fig. 1. Pretreatment with NAC and triptolide attenuated LPS/D-GalN-induced mortality and acute liver injury in C57BL/6 mice. NAC ($n = 14$) was injected i.p. 1 h and triptolide ($n = 9$) was given i.g. 12 h before coinjection with a lethal dose of LPS (5 μg/kg) and D-GalN (400 mg/kg). The mice of vehicle group ($n = 6$) were administered intragastrically (i.g.) with 2.5 μl/kg DMSO, 0.1% in normal saline, at 12 h before subsequent coinjection with LPS and D-GalN. A: Survival rate was measured after injection. The log-rank test was performed for survival curve. Pretreatment with NAC and triptolide attenuated LPS/D-GalN-induced acute liver injury in C57BL6 mice. Serum samples were collected 0, 2, 4, and 5 h after injection with LPS and D-GalN, and serum ALT (B) and AST (C) activity was determined. Data were expressed as the mean ± SE derived from triplicate experiments. Asterisks indicated values significantly different ($^{*}P < 0.05$, $^{**}P < 0.01$) from LPS/D-GalN group. Repeated measures of ANOVA followed by Dunnet's test were performed for B and C. [Color figure can be seen in the online version of this article, available at http://wileyonlinelibrary.com/journal/jcb]

expression patterns of the four groups. In total, 90 significantly changed spots were found (>1.5-fold difference) and 44 of these proteins (48.9%) were identified. The identified proteins are listed in Table III.

To understand the regulatory mechanisms that contributed to the effect of triptolide on severe liver injury, we used bioinformatics tools to extract and generate the most currently available information about the 44 proteins mentioned above. The proteins were grouped according to their functions using the database of Mus musculus Gene Ontology Assignments. As shown in Figure 4B, 12 protein spots were found to be associated with oxidative stress, 10 protein spots were found to be related with mitochondria, indicating that these biological processes might be targeted during ROS regulation.

TRIPTOLIDE ALTERED MAP KINASES AND NF-κB ACTIVATION

Proteomics analysis demonstrated that a variety of signaling molecules such as mitogen-activated protein kinases (MAP kinases) and NF-κB were activated in LPS-induced severe liver injury, which in turn induced the production of inflammatory cytokines and led to

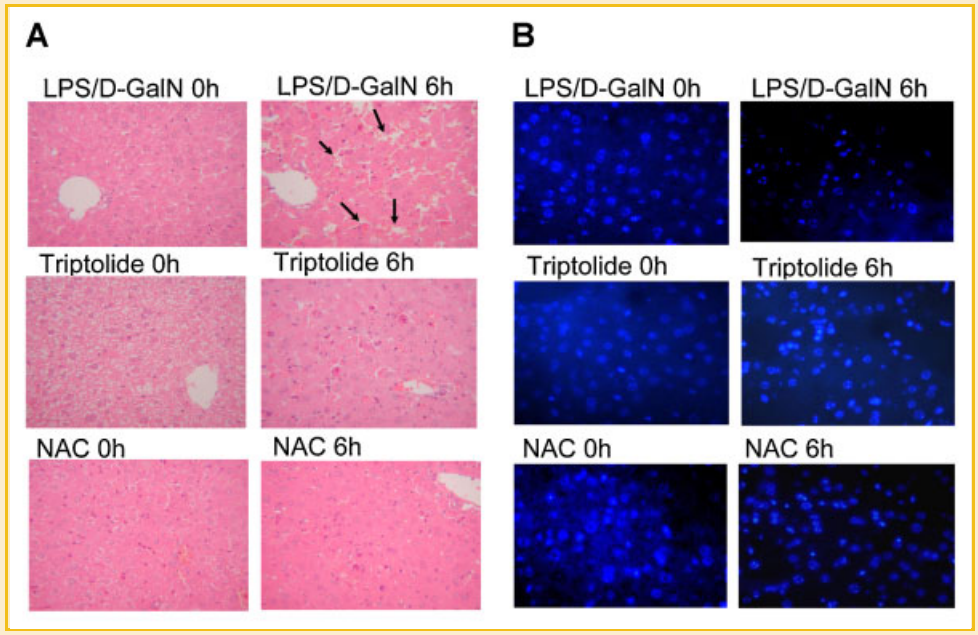

Fig. 2. Pretreatment with NAC and triptolide inhibited LPS/D-GalN-induced severe liver injury and cell death in C57BL/6 mice. NAC was injected i.p. 1 h and triptolide was given i.g. 12 h before LPS/D-GalN injection, and liver samples were collected at 0 and 6 h after coinjection with LPS and D-GalN, histologically analyzed with hematoxylin–eosin stained liver sections. The arrows indicated destruction of liver structure and the liver necrosis (A), and analyzed with Hoechst 33258-stained sections of liver (B). The results were representative of three independent experiments. [Color figure can be seen in the online version of this article, available at http://wileyonlinelibrary.com/journal/jcb]

severe liver injury [Jiang et al., 2005]. So we investigated the effects of triptolide on signaling pathways along LPS/kinase axis, which included kinetic process of phosphorylation of MAP kinases and activation of NF-κB.

As shown in Figure 5A, the combination of NF-κB with specific probes was decreased in triptolide-pretreated mice, which indicated that triptolide pretreatment caused a significant reduction in NF-κB activation in mice's livers. NAC pretreatment exhibited similar inhibition effect (Fig. 5A). IκB is the inhibitor of NF-κB, and activation of NF-κB is usually accompanied with IκB phosphorylation. Western blotting results (Fig. 5B) proposed that triptolide pretreatment significantly inhibited the phosphorylation of IκB in mice's liver. Similar results were observed in NAC-pretreated mice liver (Fig. 5B). To further confirm the results, we detected the phosphorylation of IκB by immunohistochemiscal assay (IHC) in liver tissue. IHC results were similar to Western blotting results, which showed the reduced number of p-IκB positive cells in livers (Fig. 5C). These results suggested that ROS production is an upstream event to NF-κB activation, and triptolide attenuated NF-κB activation by suppressing ROS production in mice's liver.

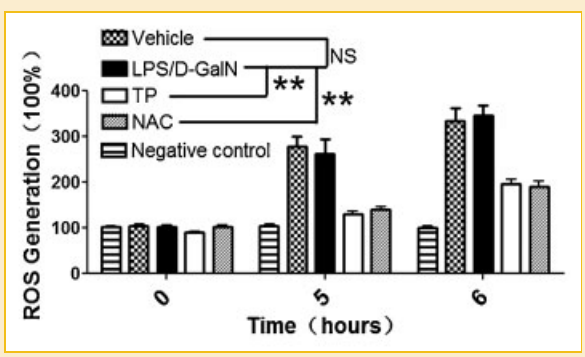

Fig. 3. Pretreatment with NAC and triptolide attenuated LPS/D-GalN-induced ROS in C57BL/6 mice's liver. NAC was injected i.p. 1 h and triptolide was given i.g. 12 h before LPS/D-GalN injection. The mice of vehicle group were administered intragastrically (i.g.) with 2.5 μl/kg DMSO, 0.1% in normal saline, at 12 h before subsequent coinjection with LPS and D-GalN. Liver samples were collected at 0, 5, and 6 h, and ROS level in livers were determined by the fluorescence probe DHR. The relative amount of ROS level was expressed as the fluorescence ratio of the treatment to control. The results were representative of three independent experiments. Asterisks denoted a response that was significantly different from LPS/D-GalN group ($^{**}P < 0.01$). Repeated measures of ANOVA followed by Dunnet's test were performed.

The activation of JNK and p38 were markedly attenuated by triptolide-pretreated mice as shown in Figure 6. NAC pretreatment exhibited a similar inhibitory effect (Fig. 6). These results were supported by IHC which showed that triptolide or NAC pretreatment decreased the number of p-JNK positive cells in livers (Fig. 6B). These results indicate that triptolide can attenuate JNK and p38 activation by suppressing ROS production in mice's livers. On the other hand, after triptolide pretreatment, the activation of ERK was prolonged from 2 to 5 h, but NAC pretreatment did not have any obvious effect on ERK activation, suggesting that the activation of ERK may have a protective effect on LPS-induced severe liver injury and triptolide can protect the animal from oxidative stress by prolonging the activation of ERK.

Thus, we proposed that triptolide could induce the phosphorylation of ERK. To explore the dynamic mechanism of ERK phosphorylation, we constructed a simplified model which covered the essential interactions in MAPK network. In "untreated" cells, in

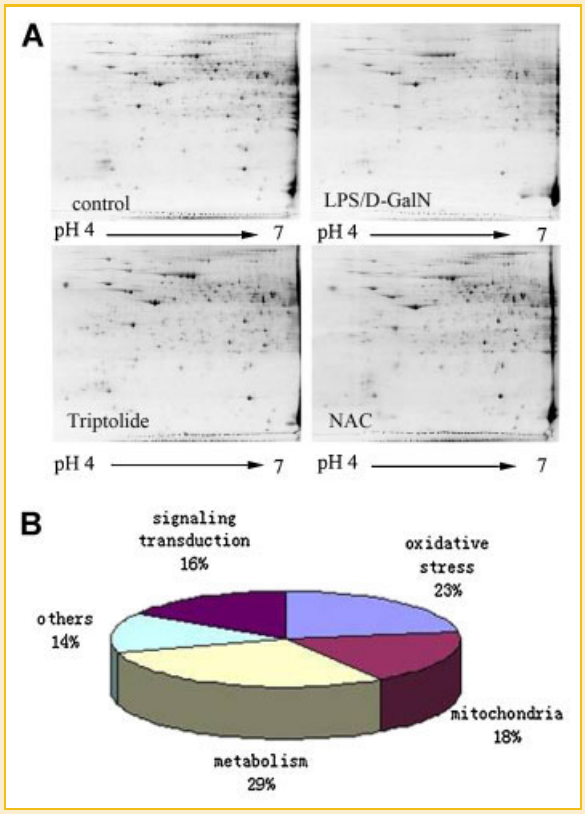

Fig. 4. Liver protein variation profiles were obtained using proteomics. A: Image of 2-D polyacrylamide gel stained with Coomassie Blue R-250. The four groups included negative control, LPS plus D-GalN treated group, NAC group which was injected i.p. 1 h before LPS/D-GalN injection, triptolide group which was given i.g. 12 h before LPS/D-GalN injection, and liver samples were collected 6 h. Proteins were extracted in livers from each group and then subjected to 2-DE. B: Cluster grouping of 44 proteins identified by mass spectrometry according to their functions. [Color figure can be seen in the online version of this article, available at http://wileyonlinelibrary.com/journal/jcb]

silico simulation did confirm the dynamics of P-ERK (compare Fig. 6A with Fig. 7, left). When phosphorylation rates were down-regulated (i.e., triptolide treated group), we found that the simulation result recapitulated the experimentally observed patterns (compare Fig. 6A with Fig. 7, right). Furthermore, we found that inhibition of P-ERK dephosphorylation (i.e., lower k9 and k10, only a fourfold reduction was needed to recapitulate the experimentally observed ERK activation events, also see Table II) was much more efficient than inducing the phosphorylation (i.e., increase k7 and k8, where at least a 1000-fold increase in phosphorylation rates was required, data not shown). Taken together, we proposed that triptolide probably induced ERK phosphorylation through inhibiting its dephosphorylation rates.

DISCUSSION

Oxidative stress, characterized by an excess of ROS, has been shown to be involved in the pathogenesis of a variety of liver diseases [Bomzon and Ljubuncic, 2001; Zhao et al., 2008]. In LPS/D-GalN-induced severe liver injury model, mice often die within a couple of days, as observed in our study, due to a rapid production of toxic ROS after LPS/D-GalN intoxication. In the study of Liu et al. [2008], the ROS inhibitor such as Baicalin and anti-oxidant NAC was shown to protect mice from endotoxin shock induced by LPS/D-GalN, since less ROS and inflammatory cytokines were generated on that condition, compared with the LPS/D-GalN only treated group.

Recently, several studies revealed that triptolide could regulate the oxidative stress imbalance [Wu et al., 2006; Zhou et al., 2006], which suggested that triptolide might be used as a potential anti-oxidative modulator for liver injury research. Considering that LPS/D-GalN-induced severe liver injury model has been well established, we used this model in order to evaluate the anti-oxidant capacity of triptolide in vivo. In this model, LPS/D-GalN was used as an inducer of oxidative stress and subsequent liver injury. The result showed that the mice treated with LPS/D-GalN died in the short span of time and the salvage effect was not obvious with post treatment of triptolide (data not show). Therefore, we chose the pretreatment of triptolide as the method of drug delivery. Triptolide was used by oral administration (i.g.) to simulate route of Tripterygium administration in traditional Chinese medicine [Kizelsztein et al., 2009].

In the damaged liver model, the balance between ROS generation and elimination was disrupted and resulted in the production of substantially high level of ROS, which would lead to the shift of redox status in liver. The redox imbalance might significantly reduce the ability to cope with oxidative stress, resulting in the breakdown of anti-oxidant defense system in the animal. As the results displayed by proteomes, the anti-oxidant defense system was damaged in mice livers and triptolide pretreatment rescued the destroyed anti-oxidant defense system (Table III), further confirming that the salvage effect of triptolide on severe liver injury was associated with its anti-oxidative activity. As calculated by the molar amount of component per body mass, the administered dose of triptolide was 1.8×10^{-8} mol/kg (5 μg/kg), while NAC was 9.2×10^{-4} mol/kg (150 mg/kg). There was a ~60,000-fold difference. Therefore, it is highly unlikely that triptolide acts through similar mechanisms as ROS scavengers.

Among the proteins that displayed altered expression through LPS/D-GalN and/or triptolide pretreatment exposure, five functional groups were identified by proteomics, including unknown function (Fig. 4). Among the oxidative stress related proteins peroxiredoxin-1 and oxidoreductase, regarded as the negative regulators of ROS, were down-regulated in the liver injury group, and their levels were partly recovered following the triptolide pretreatment. In addition, we found that another anti-oxidant enzyme-thioredoxin was up-regulated 4.6-fold in the liver injury group, and the up-regulation was 9.0-fold higher after triptolide pretreatment. These results demonstrate that the increase of thioredoxin expression with pretreatment of triptolide was large enough to reduce the ROS level and salvage the liver injury.

From the large scale of proteomic information, we also found proteins which have significant changes (increased by 150% or decreased by 50%) between LPS/D-GalN group and triptolide pretreatment group (Table III). For example, regucalcin protein was

TABLE III. Protein Abundance Changes in Mouse Liver as Determined by MALDI-TOF Spectrometer From 2-D Gels

Regulation	Protein name	Accession no.[a]	Ratio LPS/D-GalN[b]	Ratio triptolide[c]	Ratio NAC[d]
Down[e]	Lactoylglutathione lyase	Q9CPU0	1.40199	0.548366	1.528405
Down	Heat shock cognate 71 kDa protein	P63017	1.527205	0.664119	0.295074
Down	Regucalcin	Q64374	2.629911	0.666347	0.421656
Down	Sorbitol dehydrogenase	Q64442	1.81683	0.666648	0.677597
Down	Short-chain specific acyl-CoA dehydrogenase	Q07417	1.28017	0.463246	0.777606
Up[f]	Peroxiredoxin-1	P35700	0.200443	2.303982	5.503894
Up	Protein DJ-1	Q99LX0	0.135674	2.987691	2.932102
Up	Proteasome activator 28-alpha subunit	P97371	0.418998	2.515773	3.395252
Up	Thioredoxin	P10639	4.624049	1.94889	2.489411
Up	Purine nucleoside phosphorylase	P23492	0.422593	2.967195	2.060675
Up	14-3-3 protein epsilon	P62259	0.777202	2.148284	2.31621
Up	14-3-3 protein gamma	P61982	0.773041	1.940065	0.182422
Up	Probable oxidoreductase	Q9CXN7	0.39473	2.364024	2.807068
Up	Histidine triad nucleotide-binding protein 1	P70349	0.150846	8.880991	8.538722
Up	Pterin-4-alpha-carbinolamine dehydratase	P61458	0.911214	1.578628	1.316684
Up	Adenosylhomocysteinase	P50247	0.563492	1.772211	2.231098
Up	Fructose-1,6-bisphosphatase 1	Q9QXD6	0.563059	1.538123	1.566907
Up	Formimidoyltransferase-cyclodeaminase	Q91XD4	0.516947	1.981207	2.047984
Up	T-complex protein 1 subunit epsilon	P80316	0.259456	3.588643	2.189477
Up	Calreticulin precursor	P14211	0.53181	1.570743	3.321039
Up	Epoxide hydrolase 2	P34914	0.520209	2.512665	2.204445
Up	Carbamoyl-phosphate synthase	Q8C196	0.16854	2.095597	2.832538
Up	Heat shock 70 kDa protein 9	P38647	0.356823	1.582614	1.929534
	Alpha-enolase	P17182	0.349178	1.34422	2.348055
	Peroxiredoxin-6	O08709	1.119265	1.150845	1.049309
	Indolethylamine *N*-methyltransferase	P40936	0.924411	1.382672	1.319344
	Annexin A5	P48036	1.193809	1.222324	1.106474
	14-3-3 protein zeta/delta	P63101	2.136272	1.229522	1.352825
	Cytochrome b5	P56395	3.543098	0.746222	0.411035
	Selenium-binding protein 2	Q63836	0.294609	1.390538	2.050647
	D-dopachrome decarboxylase	O35215	1.24486	0.948887	0.849133
	Heat shock protein HSP 90-alpha	P07901	0.854444	1.381336	1.572894
	Ubiquinol-cytochrome *c* reductase complex core protein I	Q9CZ13	0.459233	0.989038	3.896608
	Serum albumin precursor	P07724	0.877621	1.256824	1.601885
	Ornithine aminotransferase	P29758	0.917752	1.097845	1.300718
	Pyruvate kinase isozyme M2	P52480	1.449377	0.87638	0.891597
	60 kDa heat shock protein	P63038	1.937828	1.084246	0.466554
	Aldehyde dehydrogenase	P47738	1.236228	0.823961	0.910773
	Phenylalanine-4-hydroxylase	P16331	0.877435	1.033644	1.127257
	Adenosine kinase	P55264	0.51131	0.998107	2.346367
	10-Formyltetrahydrofolate dehydrogenase	Q8R0Y6	1.112801	1.121492	1.040074
	Selenium-binding protein 1	P17563	0.720593	0.773904	1.652873
	Ketohexokinase	P97328	0.622792	0.788327	1.525903
	Major urinary protein 3 precursor	P04939	0.875826	1.271089	1.256405

[a]Accession number in NCBI, SWISS-PROT.
[b]Protein expression ratios of (LPS/D-GalN)/negative control.
[c]Protein expression ratios of Triptolide/(LPS/D-GalN).
[d]Protein expression ratios of NAC/(LPS/D-GalN).
[e]Protein expression ratios of Triptolide/(LPS/D-GalN) less than 0.67.
[f]Protein expression ratios of Triptolide/(LPS/D-GalN) more than 1.5.

up-regulated by LPS pretreatment because when liver cells were injured by LPS, the increase in regucalcin expression might protect the cells from apoptosis and hypoxia [Yamaguchi, 2000]. The pretreatment of triptolide or NAC made the compensatory increase in the expression of regucalcin return to normal level. Sorbitol dehydrogenase, another biomarker of hepatic response, was decreased because it was released into the serum by liver injury [Amacher, 2002]. Compared with the decreased proteins, the amount of increased proteins after triptolide pretreatment were much more, such as 14-3-3 protein and histidine triad nucleotide-binding protein 1 (Table III). 14-3-3 Proteins interacted with over 100 proteins and thereby participated in many cellular functions, including mediating oxidative stress signaling [Goldman et al., 2004]. Histidine triad nucleotide-binding protein 1, also designated PKC-interacting protein (PKCI), belonged to PKC inhibitors family [Su et al., 2003]. In the study of Saberi et al. [2008], PKC inhibitors were effective in reducing necrosis caused by H_2O_2 (80%), so histidine triad nucleotide-binding protein 1 might be one of effecter molecules to the triptolide.

We found that triptolide pretreatment attenuated NF-κB activation in damaged liver (Fig. 5). Many studies explored that NF-κB was a redox-sensitive and oxidant-activated transcription factor, which regulated inflammation-related gene expression and in turn led to tissue and organ damage [Simmonds and Foxwell, 2008]. Our previous report also revealed that the suppressive effect of triptolide on macrophages was associated with its suppressing on the generation of ROS and NF-κB activation [Wu et al., 2006]. These results suggested the possibility that in severe liver injury triptolide firstly protected the anti-oxidant defense system from destruction, which in turn reduced NF-κB activation and alleviated liver injury. To test this possibility, we investigated the NF-κB activation by pretreatment with NAC (Fig. 5). The result showed that pretreatment with NAC inhibited NF-κB activation in damaged liver, indicating that ROS production was an upstream event to NF-κB activation in

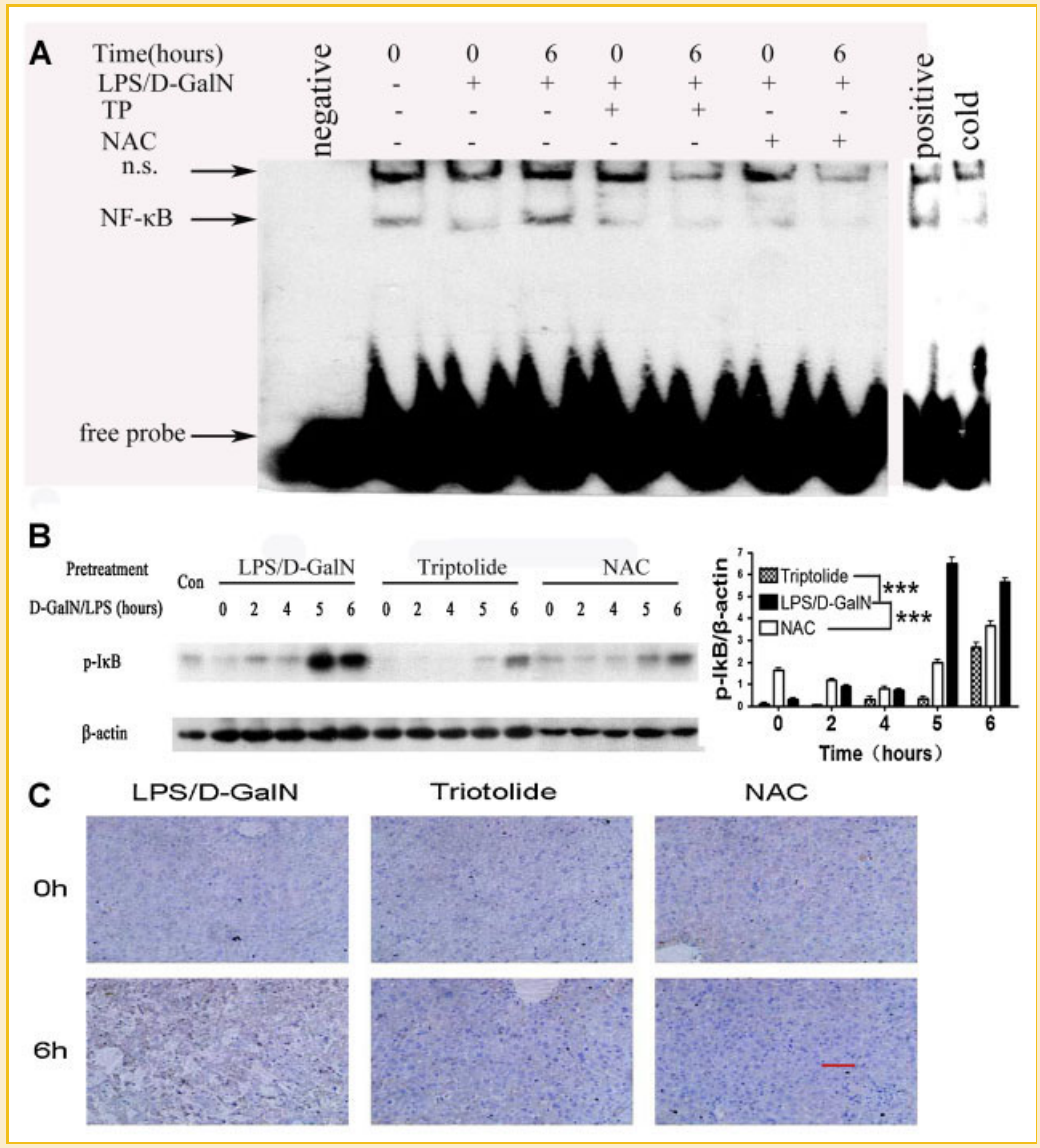

Fig. 5. Pretreatment with NAC and triptolide inhibited LPS/D-GalN-induced NF-κB activation in C57BL/6 mice's livers. NAC was injected i.p. 1 h and triptolide was given i.g. 12 h before LPS/D-GalN injection, and liver samples were collected at 0, 2, 4, 5, and 6 h. A: The activation of NF-κB was determined by EMSA, "n.s." means non-specific bands, "cold" line contained a 100-fold molar excess of unlabeled oligonucleotide. B: Phosphorylation of IκB were determined by Western blotting, semi-quantification analysis according to intensity of each band is performed. The results were representative of three independent experiments. Asterisks denoted a response that was significantly different from LPS/D-GalN group ($^{***}P < 0.001$). Repeated measures of ANOVA followed by Dunnet's test were performed. C: Phosphorylation of IκB were determined by immunohistochemistry. The results were representative of three independent experiments. The scale bar represents 70 μm. [Color figure can be seen in the online version of this article, available at http://wileyonlinelibrary.com/journal/jcb]

severe liver injury, and triptolide inhibited NF-κB activation by attenuating ROS level in the damaged liver.

To further confirm the inhibitory effect of triptolide on NF-κB, we examined the phosphorylation of IκB. IκB was the inhibitory molecule of NF-κB and its phosphorylation and degradation led to the activation of NF-κB. Data indicated that the inhibitory effect of triptolide on NF-κB activation was due to its inhibition on IκB phosphorylation. HSP70 is another inhibitor of NF-κB, specifically binding the coiled-coil domain of IκB kinase (IKK) to inhibit IKK activity and consequently inhibiting NF-κB-dependent gene induction [Ran et al., 2004]. Heat shock 70 kDa protein 9 which belonged to the HSP70 family was up-regulated by triptolide and NAC pretreatment (Table III), which further suggested the inhibitory effect of triptolide on NF-κB.

This study shows that triptolide can inhibit JNK and p38 MAP kinases activation and prolong ERK activation. Emerging evidences have highlighted a central role for MAP kinases family in various liver diseases, indicating that the salvage effect of triptolide on severe liver injury might be correlated with modulation on MAP kinases. Kim et al. [2004] had reported that triptolide can inhibit LPS-induced phosphorylation activation of JNK. Recent papers also proved that MAP kinases family including JNK, p38, and ERK were

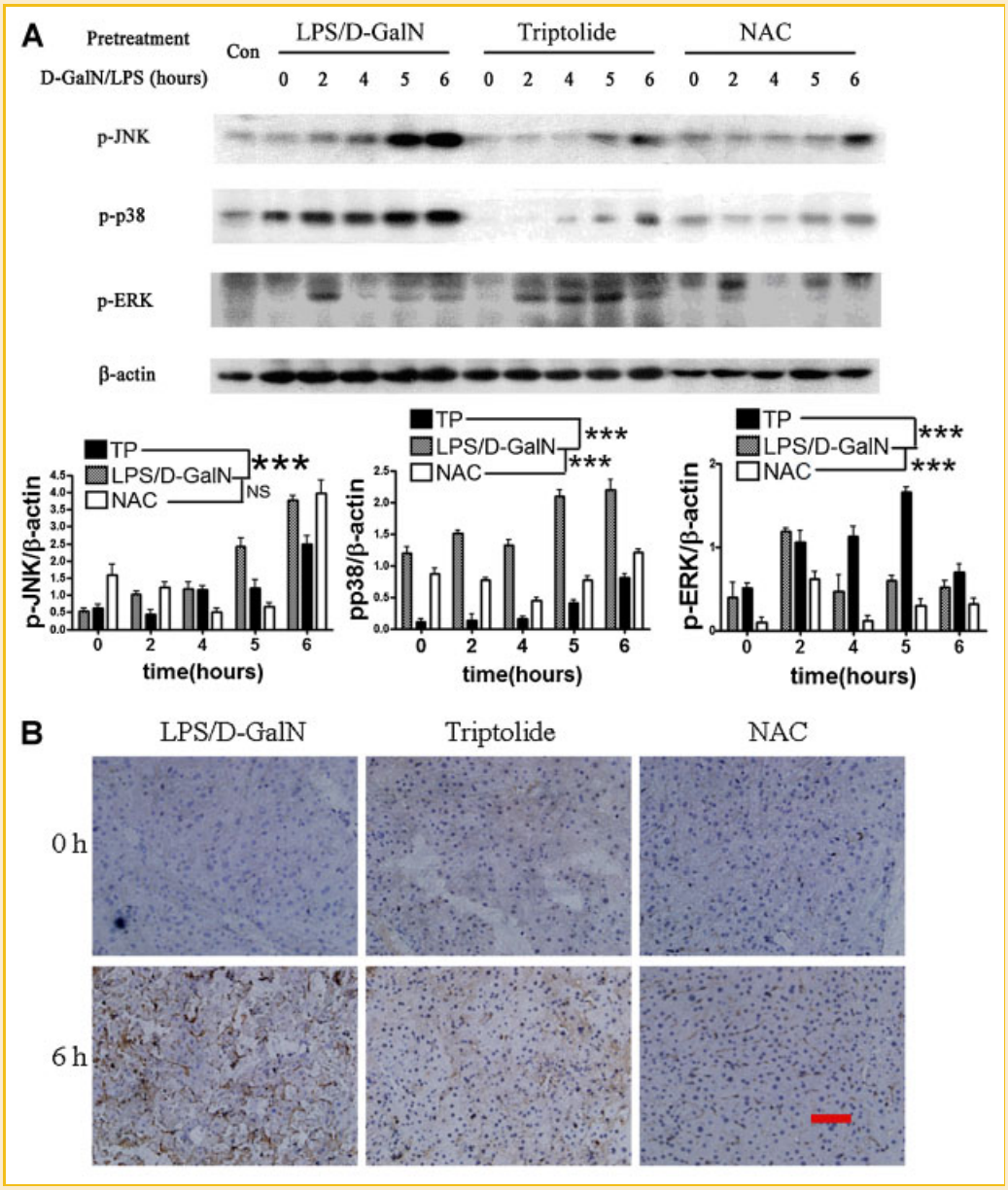

Fig. 6. Pretreatment with NAC and triptolide inhibited LPS/D-GalN-induced activation of MAPKs in C57BL/6 mice's liver. NAC was injected i.p. 1 h and triptolide was given i.g. 12 h before LPS/D-GalN injection. Liver samples were collected at 0, 2, 4, 5, and 6 h. Phosphorylation of p38 and ERK were determined by Western blotting (A), and phosphorylation of JNK was determined by Western blotting (A) and immunohistochemistry (B). The results were representative of three independent experiments. Semi-quantification analysis according to intensity of each band was performed. The results were representative of three independent experiments. Asterisks denoted a response that was significantly different from LPS/D-GalN group ($^{***}P < 0.001$). Repeated measures of two-way ANOVA followed by Dunnet's test were performed. The scale bar represents 70 μm. [Color figure can be seen in the online version of this article, available at http://wileyonlinelibrary.com/journal/jcb]

strongly activated by oxidative stress [Zhang et al., 2008], and Chiang et al. revealed that ROS was required for LPS-induced activation of p38, indicating that ROS ectopic elevation might be an upstream event of MAP kinases activation in severe liver injury [Chiang et al., 2006]. We detected this possibility by pretreatment with NAC and found that NAC effectively inhibited activation of JNK and p38, indicating that ROS production was the upstream event to activation of JNK and p38 and triptolide inhibited JNK and p38 activation by attenuating ROS production.

Pretreatment with triptolide made ERK active within a longer time span after LPS/D-GalN injection, which was different from NAC treatment sample. The activation of ERK was prolonged by triptolide in this model which indicated the role of phosphorylated ERK as a survival signal during oxidative stress [Rosseland et al., 2005]. Mathematical modeling has been applied to biological systems for a long history, and played pivotal roles in unraveling the qualitative features of signaling pathways. To further investigate the intrinsic regulatory mechanisms in MAPK pathway, we constructed a

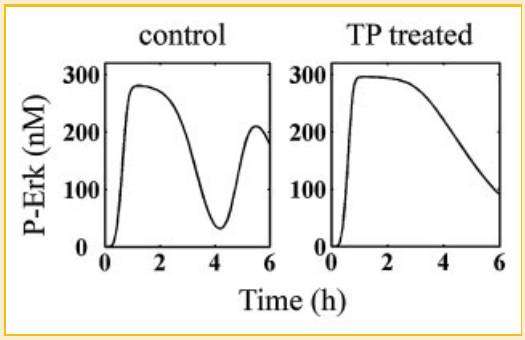

Fig. 7. The temporal responses of P-ERK activity. Left panel: Simulation of P-ERK activity (nanomolar) in untreated cells. Right panel: Simulation of P-ERK activity in Triptolide-treated cells. The computational simulation was performed within a 6-h time window in 1-min increments.

simplified mathematical model which derived from a classical model proposed by Kholodenko [2000]. Based on our mathematical model, we verified that increased phosphorylation of ERK dramatically altered the dynamical pattern which was consistent with experimental results (compare Fig. 6A and Fig. 7). The congruence between mathematical model and experiments did validate our model construction. Furthermore, by tuning the parameters, we identified that changing dephosphorylation rate might be a more sensitive way in obtaining the experimentally observed P-ERK patterns, and therefore argued that triptolide might augment the phosphorylation by attenuating the dephosphorylation rates. Further experiments are needed to discriminate these possibilities.

CONCLUSIONS

The results from this study provide direct evidence, that for the first time, triptolide can protect liver cells from oxidative stress. Moreover, the anti-oxidative role of triptolide on severe liver injury in vivo may be related with its inhibition on NF-κB and MAPK activation. Our data may aid in developing more effective strategies and application of triptolide analogues in the clinical trials.

ACKNOWLEDGMENTS

This study was supported by the National Natural Science Foundation of China (nos. 81001665, 91013015, 30821006, 30870588), partially supported by National Key Basic Research Program of China (no. 2010CB912203). The authors thank N. Pachikara (University of Medicine and Dentistry of New Jersey) for grammatical correction of the manuscript.

REFERENCES

Amacher DE. 2002. A toxicologist's guide to biomarkers of hepatic response. Hum Exp Toxicol 21:253–262.

Bomzon A, Ljubuncic P. 2001. Oxidative stress and vascular smooth muscle cell function in liver disease. Pharmacol Ther 89:295–308.

Brinker AM, Ma J, Lipsky PE, Raskin I. 2007. Medicinal chemistry and pharmacology of genus Tripterygium (Celastraceae). Phytochemistry 68: 732–766.

Chen T, Wang QS, Cui J, Yang W, Shi Q, Hua ZC, Ji JG, Shen PP. 2005. Induction of apoptosis in mouse liver by microcystin-LR—A combined transcriptomic, proteomic, and simulation strategy. Mol Cell Proteomics 4:958–974.

Chiang E, Dang O, Anderson K, Matsuzawa A, Ichijo H, David M. 2006. Cutting edge: Apoptosis-regulating signal kinase 1 is required for reactive oxygen species-mediated activation of IFN regulatory factor 3 by. lipopolysaccharide. J Immunol 176:5720–5724.

Galanos C, Freudenberg MA, Reutter W. 1979. Galactosamine-induced sensitization to the lethal effects of endotoxin. Proc Natl Acad Sci USA 76:5939–5943.

Goldman EH, Chen L, Fu H. 2004. Activation of apoptosis signal-regulating kinase 1 by reactive oxygen species through dephosphorylation at serine 967 and 14-3-3 dissociation. J Biol Chem 279:10442–10449.

Han D, Hanawa N, Saberi B, Kaplowitz N. 2006. Mechanisms of liver injury. III. Role of glutathione redox status in liver injury. Am J Physiol Gastrointest Liver Physiol 291:G1–G7.

Ji SM, Wang QW, Chen JS, Sha GZ, Liu ZH, Li LS. 2006. Clinical trial of Tripterygium Wilfordii Hook F. in human kidney transplantation in China. Transplant Proc 38:1274–1279.

Jiang W, Sun R, Wei HM, Tian ZG. 2005. Toll-like receptor 3 ligand attenuates LPS-induced liver injury by down-regulation of toll-like receptor 4 expression on macrophages. Proc Natl Acad Sci USA 102:17077–17082.

Kholodenko BN. 2000. Negative feedback and ultrasensitivity can bring about oscillations in the mitogen-activated protein kinase cascades. Eur J Biochem 267:1583–1588.

Kim YH, Lee SH, Lee JY, Choi SW, Park JW, Kwon TK. 2004. Triptolide inhibits murine-inducible nitric oxide synthase expression by down-regulating lipopolysaccharide-induced activity of nuclear factor-kappa B and c-Jun NH2-terminal kinase. Eur J Pharmacol 494:1–9.

Kizelsztein P, Komarnytsky S, Raskin I. 2009. Oral administration of triptolide ameliorates the clinical signs of experimental autoimmune encephalomyelitis (EAE) by induction of HSP70 and stabilization of NF-kappa B/I kappa B alpha transcriptional complex. J Neuroimmunol 217: 28–37.

KretzRemy C, Mehlen P, Mirault ME, Arrigo AP. 1996. Inhibition of I kappa B-alpha phosphorylation and degradation and subsequent NF-kappa B activation by glutathione peroxidase overexpression. J Cell Biol 133: 1083–1093.

Li FQ, Lu XZ, Liang XB, Zhou HF, Xue B, Liu XY, Niu DB, Han JS, Wang XM. 2004. Triptolide, a Chinese herbal extract, protects dopaminergic neurons from inflammation-mediated damage through inhibition of microglial activation. J Neuroimmunol 148:24–31.

Liu LL, Gong LK, Wang H, Xiao Y, Wu XF, Zhang YH, Xue X, Qi XM, Ren J. 2008. Baicalin inhibits macrophage activation by lipopolysaccharide and protects mice from endotoxin shock. Biochem Pharmacol 75:914–922.

Ma J, Dey M, Yang H, Poulev A, Pouleva R, Dorn R, Lipsky PE, Kennelly EJ, Raskin I. 2007. Anti-inflammatory and immuno suppressive compounds from Tripterygium wilfordii. Phytochemistry 68:1172–1178.

Mignon A, Rouquet N, Fabre M, Martin S, Pages JC, Dhainaut JF, Kahn A, Briand P, Joulin V. 1999. LPS challenge in D-galactosamine-sensitized mice accounts for caspase-dependent fulminant hepatitis, not for septic shock. Am J Respir Crit Care Med 159:1308–1315.

Morikawa A, Koide N, Sugiyama T, Mu MM, Hassan F, Islam S, Ito H, Mori I, Yoshida T, Yokochi T. 2004. The enhancing action of D-galactosamine on lipopolysaccharide-induced nitric oxide production in RAW 264.7 macrophage cells. FEMS Immunol Med Microbiol 41:211–218.

Nogueira CW, Wilhelm EA, Jesse CR. 2009. Protective effect of p-methoxyl-diphenyl diselenide in lethal acute liver failure induced by lipopolysaccharide and d-galactosamine in mice. Fundam Clin Pharmacol 23:727–734.

Qiu D, Kao PN. 2003. Immunosuppressive and anti-inflammatory mechanisms of triptolide, the principal active diterpenoid from the Chinese medicinal herb Tripterygium wilfordii Hook f. Drugs R D 4:1–18.

Ran RQ, Lu AG, Zhang L, Tang Y, Zhu Y, Zhu HY, Xu HC, Feng YX, Han C, Zhou GP, Rigby AC. 2004. Hsp70 promotes TNF-mediated apoptosis by binding IKK gamma and impairing NF-kappa B survival signaling. Genes Dev 18:1466–1481.

Rosseland CM, Wierod L, Oksvold MP, Werner H, Ostvold AC, Thoresen GH, Paulsen RE, Huitfeldt HS, Skarpen E. 2005. Cytoplasmic retention of peroxide-activated ERK provides survival in primary cultures of rat hepatocytes. Hepatology 42:200–207.

Saberi B, Shinohara M, Ybanez MD, Hanawa N, Gaarde WA, Kaplowitz N, Han D. 2008. Regulation of H_2O_2-induced necrosis by PKC and AMP-activated kinase signaling in primary cultured hepatocytes. Am J Physiol Cell Physiol 295:C50–C63.

Savegnago L, Wilhelm EA, Jesse CR, Roman SS, Nogueira CW. 2009. Hepatoprotective effect of 3-alkynyl selenophene on acute liver injury induced by D-galactosamine and lipopolysaccharide. Exp Mol Pathol 87:20–26.

Schwabe RF, Brenner DA. 2006. Mechanisms of liver injury. I. TNF-alpha-induced liver injury: Role of IKK, JNK, and ROS pathways. Am J Physiol Gastrointest Liver Physiol 290:G583–G589.

Simmonds RE, Foxwell BM. 2008. Signalling, inflammation and arthritis—NF-kappa B and its relevance to arthritis and inflammation. Rheumatology 47:584–590.

Su T, Suzui M, Wang L, Lin CS, Xing WQ, Weinstein IB. 2003. Deletion of histidine triad nucleotide-binding protein 1/PKC-interacting protein growth in mice enhances cell growth and carcinogenesis. Proc Natl Acad Sci USA 100:7824–7829.

Tsai SL, Tai DI, Chen YM, Chuang YL, Peng CY, Sheen IS, Yeh CT, Chang KSS, Huang SN, Kuo GC, Liaw YF. 2000. Activation of nuclear factor kappa B in hepatitis C virus infection: Implications for pathogenesis and hepatocarcinogenesis. Hepatology 31:656–664.

Wang W, Yang S, Su Y, Xiao Z, Wang C, Li X, Lin L, Fenton BM, Paoni SF, Ding I, Keng P, Okunieff P, Zhang L. 2007. Enhanced antitumor effect of combined triptolide and ionizing radiation. Clin Cancer Res 13:4891–4899.

Wiesel P, Patel AP, DiFonzo N, Marria PB, Sim CU, Pellacani A, Maemura K, LeBlanc BW, Marino K, Doerschuk CM, Yet SF, Lee ME, Perrella MA. 2000. Endotoxin-induced mortality is related to increased oxidative stress and end-organ dysfunction, not refractory hypotension, in heme oxygenase-1-deficient mice. Circulation 102:3015–3022.

Wu YY, Cui J, Bao XF, Chan SP, Young DO, Liu D, Shen PP. 2006. Triptolide attenuates oxidative stress, NF-kappa B activation and multiple cytokine gene expression in murine peritoneal macrophage. Int J Mol Med 17:141–150.

Xue B, Jiao J, Zhang L, Gong Y, Xie J, Wang X. 2006. Neuroprotective effect of Tripterygium Wilfordii Hook F monomer T10 agaist hydrogen peroxideinduced PC12 cell damage and its mechanism. Chin J Neuromed 5:1194–1198.

Yamaguchi M. 2000. Minireview—Role of regucalcin in calcium signaling. Life Sci 66:1769–1780.

Zhang YH, Qi XM, Gong LK, Li Y, Liu LL, Xue X, Xiao Y, Wu XF, Ren J. 2008. Roles of reactive oxygen species and MAP kinases in the primary rat hepatocytes death induced by toosendanin. Toxicology 249:62–68.

Zhao J, Chen H, Li Y. 2008. Protective effect of bicyclol on acute alcohol-induced liver injury in mice. Eur J Pharmacol 586:322–331.

Zheng CX, Chen ZH, Zeng CH, Qin WS, Li LS, Liu ZH. 2008. Triptolide protects podocytes from puromycin aminonucleoside induced injury in vivo and in vitro. Kidney Int 74:596–612.

Zhou R, Zheng SX, Tang W, He PL, Li XY, Yang YF, Li YC, Geng JG, Zuo JP. 2006. Inhibition of inducible nitric-oxide synthase expression by (5R)-5-hydroxytriptolide in interferon-gamma- and bacterial lipopolysaccharide-stimulated macrophages. J Pharmacol Exp Ther 316:121–128.